Mechanism for thermal shrinkage of oriented polystyrene monofilaments

Yoshikazu Tanabe and Hisaaki Kanetsuna
Research Institute for Polymers and Textiles, 1-1-4 Yatabe-Higashi, Tsukuba, Ibaraki Pref. 300-21, Japan
(Received 5 February 1979; revised 2 May 1979)

Thermal shrinkage behaviour of oriented atactic polystyrene monofilaments, which show a brittle-to-ductile transition in the vicinity of $\Delta n = -2 \times 10^{-3}$ (at a temperature of 20°C and a stretching rate of 100%/min), is investigated by thermomechanical analysis (t.m.a.). The maximum contraction ratio $\Delta L_1/L_0$ at a constant rate of heating decreases linearly with increasing external tensile stress, and the limiting contraction ratio (at zero external load) has a broad maximum near the transition point. The time dependence of the isothermal contraction ratio $[\Delta L(\infty) - \Delta L(t)]/\Delta L(\infty)$ is represented by an exponential function and an Arrhenius type temperature dependence is realized with an activation energy of several tens of kcal/mol. The degree of birefringence after isothermal shrinkage ($\Delta n(\infty)$) increases linearly with an increase in external tensile load. Degrees of birefringence before isothermal shrinkage ($\Delta n(0)$) and $\Delta n(\infty)$ are related to each other almost linearly. The two-state model is effective in understanding these thermal shrinkage behaviours.

INTRODUCTION

There are two methods for fabricating the oriented atactic polystyrene monofilaments. In the first method investigated by Cleereman *et al.*[1], molten polystyrene is extruded into a bath the temperature of which is controlled within the range above the glass transition temperature T_g, and drawn simultaneously to definite extensions in a bath with the same or lower temperature and then quenched below T_g. In the second method[2], molten atactic polystyrene is extruded directly into a cooling bath or surrounding air below T_g. One of the most characteristic properties of oriented atactic polystyrene obtained by the second method is that the brittle-to-ductile transition takes place at $\sim \Delta n = -2 \times 10^{-3}$ (Δn is degree of birefringence) at a temperature of 20°C, a stretching rate of 100%/min, and with relative humidity below 65%, and that this transition point does not depend on the various spinning conditions within the range of our measurements; that is, this transition is related directly to amorphous orientation.

Amorphous orientation of these samples was investigated by wide-angle X-ray scattering experiments[3] and it turned out that the brittle-to-ductile transition is related to the packing of phenyl groups and main chains.

In this study, the thermal shrinkage behaviours of these specimens are investigated by thermomechanical analysis (t.m.a.). Cleereman *et al.*[1] and Andrews[4] have measured the isothermal retraction curves of oriented atactic polystyrene monofilaments obtained by the first spinning method. Their activation energy is very large (a few hundred kcal/mol). Ueno *et al.*[5] have observed the WLF-type superposition rule in isothermal retraction measurements on polystyrene films which were drawn above the glass transition temperature. As discussed later, the isothermal shrinkage behaviour of our polystyrene monofilaments is different from that of theirs, which suggests the existence of another thermal shrinkage mechanism for our samples. The two-state model proposed by Kambe *et al.*[6,7] is useful in the discussion of our results. Lastly, changes in the degree of birefringence before and after isothermal shrinkage are investigated based upon the same model.

EXPERIMENTAL

The sample is the commercial atactic polystyrene (Styron 679, $\bar{M}_w = 1.84 \times 10^5$, $\bar{M}_w/\bar{M}_n = 2.8$), which is spun by the same method as in the previous study[2], where the diameter of each nozzle hole is 0.5 mm and the output rate is ~1 g/min/hole. The spinning conditions such as the molten polymer temperature, the quenching temperature, the extruding conditions, the distance between nozzle and guiding roll directly under the nozzle are tabulated in *Table 1*. Two specimens (No. 1 and 2 series) were obtained under a five-hole nozzle in order to observe the effect of temperature of cooling bath. No. 3 and 4 series were extruded under a one-hole nozzle in order to investigate mainly the effect of the distance between nozzle and the guiding roll. Diameters and Δn's for these samples are denoted in *Table 2*, in which the first number for each sample shows the series number. The samples in a series were obtained by changing the winding velocity.

Table 1 Various spinning conditions of atactic polystyrene monofilaments

Sample series	Molten polymer temperature (°C)	Cooling bath and its temperature (°C)	Nozzle-roll (or surface of cooling liquid) distance (cm)
1	197	Air, 12	81
2	197	Ethanol, −68	7
3	211	Air, 10	471
4	197	Air, 23	81

0032–3861/79/091121–08$02.00

Table 2 Diameters and degrees of birefringence of specimens used in thermal shrinkage measurement

Sample	Diameter (μm)	Degree of birefringence x 10^{-3}
15	259	−0.72
17	205	−1.24
14	190	−1.61
13	154	−2.35
12	104	−5.23
11	72.8	−9.56
16	61.0	−12.8
25	272	−0.82
24	211	−1.32
27	183	−1.66
23	163	−2.20
22	122	−4.02
21	88.6	−6.75
26	71.4	−10.48
310	281	−0.23
34	156	−0.829
33	129	−1.34
32	95.6	−2.51
31	73.8	−4.26
36	59.8	−5.55
37	50.2	−8.48
39	48.0	−9.02
45	284	−1.16
44	183	−3.44
43	137	−5.50
42	105	−8.03
41	75.7	−13.8
46	63.1	−18.7

The thermomechanical apparatus TM-1500 (Shinku Riko Co. Ltd) with a balance-type loading was used. All measurements were made in air. For the measurement of thermal shrinkage at constant heating rate, the change in length of samples under tensile load (30 mg ~ 1 g) and its temperature were recorded simultaneously at a constant rate of heating (2°C/min). In the measurement of isothermal shrinkage curves, the temperature was raised to that required at the highest rate of heating (20°C/min) and the time dependence of length was recorded at the desired constant temperature.

RESULTS AND DISCUSSION

Thermal shrinkage at constant heating rate

A schematic t.m.a. curve of polystyrene monofilaments is shown in *Figure 1*. The contraction ratio to original length (L_0 = 11.2 mm) is defined by $(\Delta L_1/L_0) \times 100$, where ΔL_1 is the maximum contracted length as defined in *Figure 1*. Its dependence on tensile load is shown in *Figure 2* for No. 1 series, for example. It is clear that the contraction ratio decreases linearly with increasing load. The extrapolated contraction ratio to zero load (which is called here the limiting contraction ratio and denoted by

$$\lim_{Y \to 0} \frac{\Delta L_1}{L_0}$$

where Y represents the external tensile stress), depends on the degree of birefringence Δn as shown in *Figure 3*. Its limiting contraction ratio increases fairly steeply as $|\Delta n|$ increases to $\sim|-2 \times 10^{-3}|$ and decreases with an easier grade in the range of $|\Delta n| > |-2 \times 10^{-3}|$. This change in the limiting contraction ratio is not so drastic as that in elongation at break[2,3]. It is, however, interesting that the maximum value of Δn dependence of its limiting contraction ratio appears near $\Delta n = -2 \times 10^{-3}$ where brittle-to-ductile transition is observed. The effect of temperature of the cooling bath is not distinguished in *Figure 3* (see No. 1 and No. 2 samples). But influence of the molten temperature and the distance between nozzle and the guiding roll is prominent (No. 3 and No. 4 samples).

Two-state model

The two-state model, which has previously been proposed by Kambe *et al.*[6,7], is very convenient for the consideration of our results. Each molecular chain constituting the oriented amorphous state is divided into submolecules, which are assumed to occupy the contracted (α) state or extended (β) state randomly. The number of submolecules in α and β states in a chain at time t is designated by $p_\alpha(t)$ and $p_\beta(t)$, and each length of projection on the fibre axis by l_α and l_β. The total number p of submolecules in a chain and its whole length $L(t)$ at time t are given by

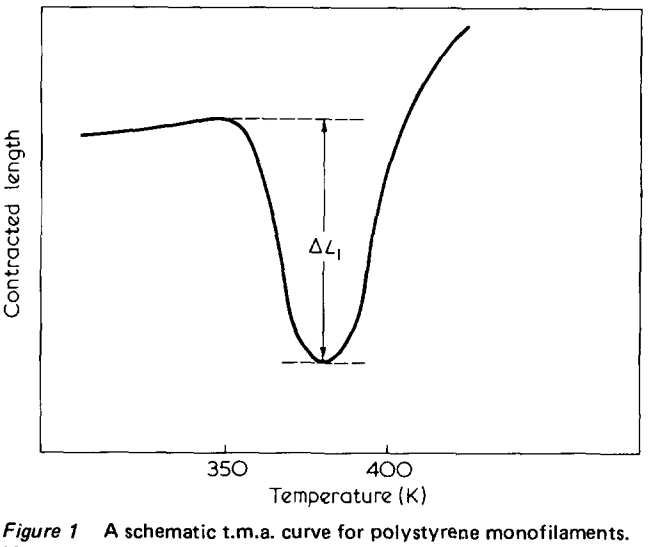

Figure 1 A schematic t.m.a. curve for polystyrene monofilaments. Maximum contracted length ΔL_1 is defined as shown in this Figure

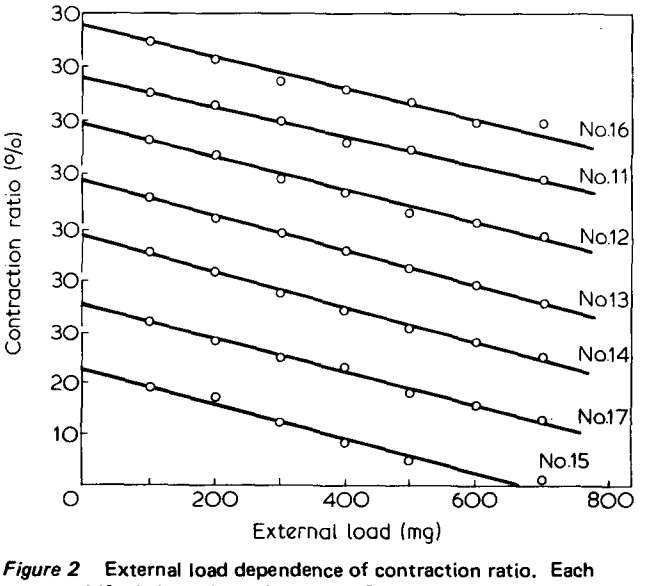

Figure 2 External load dependence of contraction ratio. Each curve is shifted along the ordinate by 10%

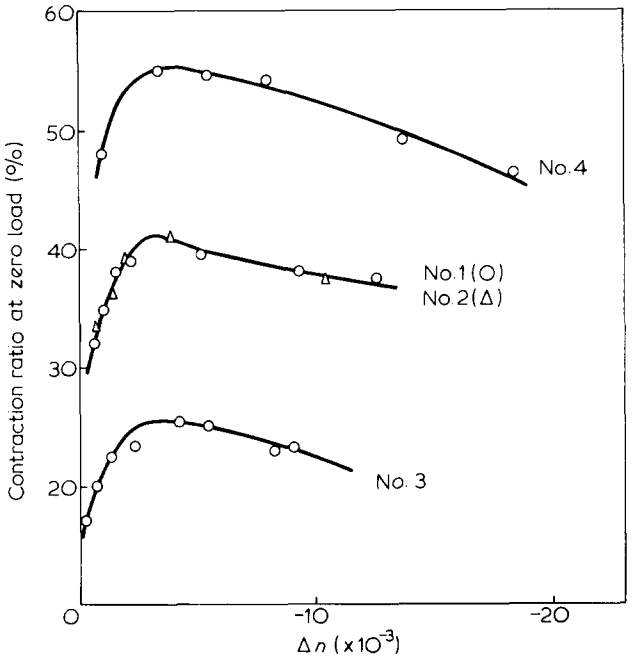

Figure 3 The limiting ratio at zero load *vs.* degree of birefringence (Δn). No. 1 series samples (○) were spun in air (+12°C) and No. 2 series samples (△) were spun in ethanol (−68°C) and the other conditions were the same for both samples. Spinning conditions for No. 3 and No. 4 series samples are shown in text

$$p = p_\alpha(t) + p_\beta(t) \tag{1}$$

$$L(t) = p_\alpha(t)\cdot l_\alpha + p_\beta(t)\cdot l_\beta \tag{2}$$

where p is assumed to be constant during thermal shrinkage. At time $t = 0$, the number of submolecules in α and β states is assumed to be $p_\alpha(0) = p_{\alpha 0}$ and $p_\beta(0) = p_{\beta 0}$, and if the number fraction $x(t)$ of submolecules is changed from the extended state to the contracted state at time t, the number of submolecules in each state is $p_{\alpha 0} + p_{\beta 0}x(t)$ and $p_{\beta 0}[1 - x(t)]$. The whole contracted length of a chain $\Delta L(t) = L(0) - L(t)$ is given by $\Delta L(t) = \Delta l \cdot p_{\beta 0} \cdot x(t)$, where $\Delta l = l_\beta - l_\alpha$, and then

$$\frac{\Delta L(t)}{L_0} = C\cdot x(t) \tag{3}$$

where

$$L_0 = L(0) = p\cdot l_\alpha + p_{\beta 0}\cdot \Delta l$$

$$C = \left[1 + (1 + c_0)\frac{l\alpha}{\Delta l}\right]^{-1}$$

and

$$c_0 = p_{\alpha 0}/p_{\beta 0}$$

assuming that the contracted length of an oriented amorphous monofilament is proportional to the contracted length of its constituting molecular chain, the observed contraction ratio is expressed by equation (3). Under the assumption of the first order reaction, the contraction rate is represented by equation (4).

$$\frac{dp_\alpha(t)}{dt} = k_f p_\beta(t) - k_b p_\alpha(t) \tag{4}$$

where k_f and k_b are the reaction constants for the forward and backward reactions, respectively, as shown in *Figure 4*, and given as follows:

$$k_f = A\exp\left(-\frac{\Delta E + Y\cdot s_0\cdot \Delta l}{RT}\right) \tag{5}$$

$$k_b = A\exp\left(-\frac{\Delta E + \epsilon - Y\cdot s_0\cdot \Delta l}{RT}\right) \tag{6}$$

and ΔE is the activation energy, ϵ is the energy difference between α state and β state, s_0 is the cross section of a submolecule, R is the gas constant, T is the absolute temperature and A is a proportional factor. All the thermal shrinkage behaviours of the two state model are described by solving equation (4).

For the case of constant heating rate, the conditions that $x = 0$ at time $t = 0$ (and temperature $T = T_0$ at which contraction begins) and $dx/dt = 0$ at time $t = t_1$ (and temperature $T = T_1$ at which contraction ends and drawing occurs) are used. The amount of contraction at time $t = t_1$ is denoted by ΔL_1 (see *Figure 1*) and, if the external stress is small enough ($Ys_0, \Delta l/RT_1 \ll 1$), the contraction ratio at time t_1 is given by (see Appendix):

$$\frac{\Delta L_1}{L_0} = \left(\lim_{Y\to 0}\frac{\Delta L_1}{L_0}\right) - \left(\frac{2K\cdot s_0\cdot \Delta l}{RT_1}\right)Y \tag{7}$$

where

$$\lim_{Y\to 0}\frac{\Delta L_1}{L_0} = C\left[1 - \frac{1 + c_0}{\left\{1 + \exp\left(\frac{\epsilon}{RT_1}\right)\right\}}\right] \tag{8}$$

and

$$K = C(1 + c_0)\frac{\exp\left(\frac{\epsilon}{RT_1}\right)}{\left\{1 + \exp\left(\frac{\epsilon}{RT_1}\right)\right\}^2} \tag{9}$$

The contraction ratio decreases linearly as external load increases, which qualitatively coincides with our experimental results in *Figure 2*.

In order to investigate the effect of various parameters we have solved equation (4) exactly and made numerical calculations. Exact solution for the contraction ratio is described by (see Appendix)

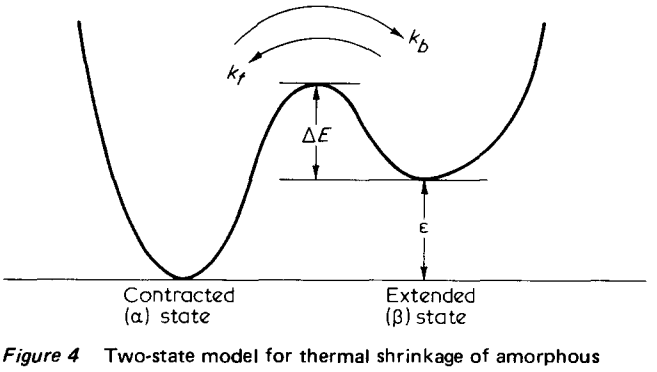

Figure 4 Two-state model for thermal shrinkage of amorphous polymers

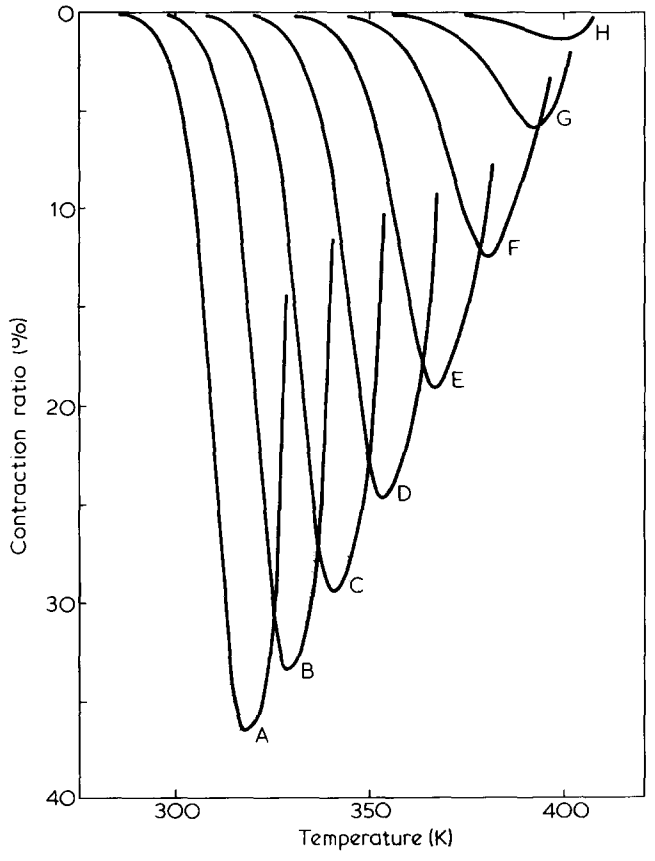

Figure 5 Effect of parameter A on the contraction ratio at zero load. ϕ = 1/30°C/sec; ΔE = 40 kcal/mol; ϵ = 4.0 kcal/mol; c_0 = 150; A (sec^{-1}) = A, 10^{26}; B, 10^{25}; C, 10^{24}; D, 10^{23}; E, 10^{22}; F, 10^{21}; G, 10^{20}; H, 10^{19}

$$\frac{\Delta L(T)}{L_0} = C\left\{\int_{T_0}^{T} Q(T')\exp\left[\int_{T_0}^{T'} P(T'')dT''\right]dT'\right\} \exp\left[-\int_{T_0}^{T} P(T)dT\right] \quad (10)$$

where $\phi = dT/dt$, $P(T) = \phi^{-1}(k_f + k_b)$ and $Q(T) = \phi^{-1}(k_f - c_0 k_b)$. The heating rate ϕ is 1/30 (°C/sec) experimentally and C is assumed to be 0.5. The value of C can be determined experimentally within the framework of the two-state model, which is discussed later. It must be noted that C is not a constant in relation to c_0 or $p_{\beta 0}$. External load Y is set to zero. Some results of numerical calculations of equation (10) are shown in *Figures 5, 6, 7* and *8*. From *Figures 5* and *6* it is apparent that parameters A and ΔE influence the curvatures of contraction curves as well as the temperature position of maximum contraction ratio. The values of $A = 10^{21}$ (sec^{-1}) and ΔE = 40 (kcal/mol) are fitted best with experimental data. This value of activation energy ΔE coincides fairly well with that obtained from the heating rate dependence of t.m.a. according to the method of Kambe *et al.* On the other hand, the parameters ϵ and c_0 influence mainly the absolute values of contraction ratio as seen in *Figures 7* and *8*.

For the discussion of the Δn dependence of the limiting contraction ratios shown in *Figure 3*, two parameters c_0 (or $p_{\beta 0}$) and ϵ should be considered in equation (8). As degree of birefringence Δn increases, $p_{\beta 0}$ increases and so c_0 decreases monotonically, and thus the limiting contraction ratio would become larger if only c_0 changes. The energy difference ϵ is nearly constant in the brittle region ($|\Delta n| \leqslant |-2 \times 10^{-3}|$) but decreases in the ductile region ($|\Delta n| \geqslant |-2 \times 10^{-3}|$) as $|\Delta n|$ increases. The reason is as follows. The energy difference ϵ is considered to be the sum of intra- and intermolecular energy. The intramolecular energy ϵ_{intra} is almost independent of degree of orientation of surrounding submolecules. Intermolecular energy ϵ_{inter} depends strongly upon it. In the brittle region the number of submolecules $p_{\beta 0}$ in extended state is small and interaction among submolecules remains the same as it is in the unoriented amorphous state[3]. Therefore, ϵ is maintained almost constant independent of intermolecular orientation. In the ductile region the degree of orientation of surrounding submolecules is higher[3] and intermolecular energy ϵ_{inter} increases in absolute value, where ϵ_{inter} is negative. Increase in ϵ_{inter} in absolute value leads to a decrease in ϵ. From the above-mentioned consideration, it is clear that in the brittle region c_0 decreases and ϵ is nearly constant and so the limiting contraction ratio increases with increase in $|\Delta n|$. In the ductile region, both c_0 and ϵ decrease with increase in $|\Delta n|$ but the effect of ϵ is prominent. Accordingly the limiting contraction ratio decreases slowly as $|\Delta n|$ increases. Although the numerical values of c_0 are not certain because the c_0 dependence of C is neglected here, it is demonstrative to interpret the Δn dependence of the limiting contraction ratios using the numerical values of various parameters. In the case of No. 3 samples, for example, ϵ is kept constant at

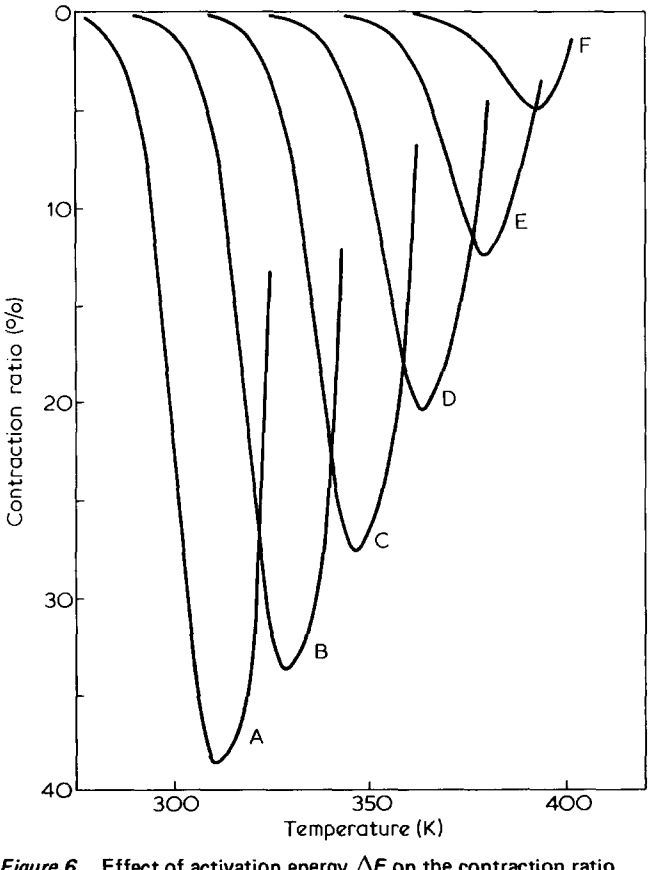

Figure 6 Effect of activation energy ΔE on the contraction ratio at zero load. $A = 10^{21}$ sec^{-1}; ϕ = 1/30 (°C/sec); ϵ = 4.0 kcal/mol; C_0 = 150. ΔE (kcal/mol); A, 32; B, 34; C, 36; D, 38; E, 40; F, 42

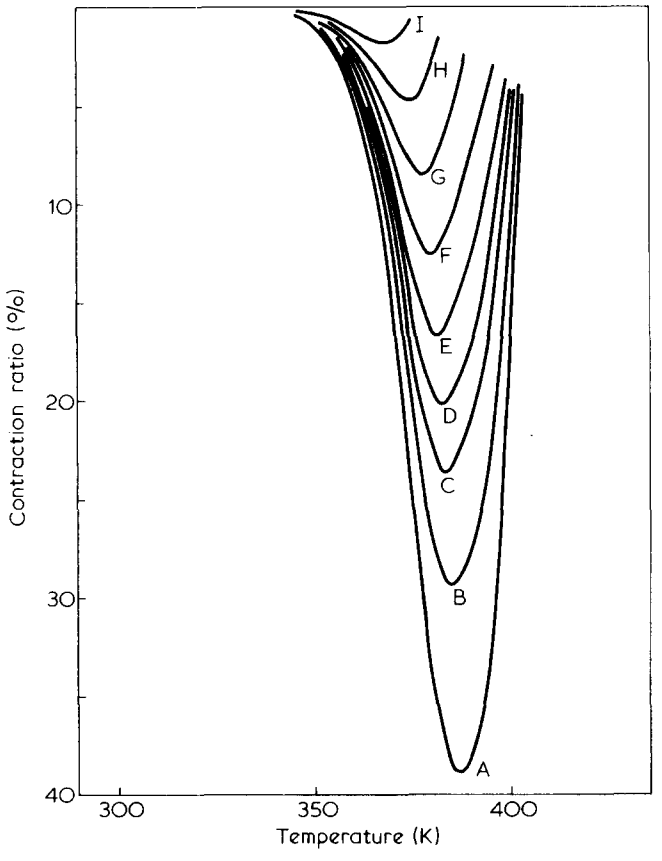

Figure 7 Effect of energy difference ϵ between the extended and the contracted states on the contraction ratio at zero load. A = 10^{21} (sec^{-1}); ϕ = 1/30 (°C/sec); ΔE = 40 kcal/mol; C_0 = 150. ϵ(kcal/mol): A, 5.0; B, 4.5; C, 4.3; D, 4.2; E, 4.1; F, 4.0; G, 3.9; H, 3.8; I, 3.7

~ 4 kcal/mol in the brittle region and c_0 changes from ~180 (for $\Delta n = -0.23 \times 10^{-3}$) to ~140 (near the transition point), and therefore the limiting contraction ratio changes from ~7 to 15%. In the ductile region, c_0 also decreases, for example, to ~50 which would lead the limiting contraction ratio to ~36%, but the decrease of ϵ from 4 kcal/mol to 3.8 kcal/mol reduces it to ~12%.

The difference of the limiting contraction ratio among No. 3, No. 4 and No. 1 and No. 2 series samples in *Figure 3* is due to the differences in frozen strain energy. In the two-state model, the contribution of frozen strain energy is involved in the energy difference ϵ per submolecule. A comparatively smaller change in ϵ results in a larger change in its contraction ratio as shown in *Figure 7*. One of the most important factors for the difference between No. 3 series and No. 4 series samples is the difference of the distance between the nozzle and the guiding roll directly under the nozzle. If the output rate and the winding velocity are the same on spinning, the average velocity gradient parallel to the flow direction in the nozzle becomes smaller as the distance between the nozzle and the guiding roll becomes larger. The smaller average velocity gradient at vitrification of molten polystyrene makes the frozen strain energy in polystyrene monofilaments smaller. Differences in the contraction ratio between No. 4 series and No. 1 or No. 2 series is due to the fact that on spinning of No. 4 series the one-hole nozzle was used and the output rate (~1 g/min) was obtained with no gear pumps but on spinning of No. 1 or No. 2 series the five-hole nozzle and gear pump were used. The frozen strain energy is very sensitive to stress distribution in molten state just before vitrification.

As shown in *Figure 3* (No. 1 and No. 2 series), the effect of the temperature of the cooling bath is not observed. Therefore, if the temperature of the cooling bath is kept between −70° and +10°C which is lower than glass transition temperature, it does not influence the frozen strain energy.

Isothermal shrinkage

Logarithm of a contraction ratio $[\Delta L(\infty) - \Delta L(t)]/\Delta L(\infty)$ under the constant tensile load (100 mg) *vs.* time in isotherma shrinkage of No. 11 sample is shown in *Figure 9*. The temperature maintained is shown. In this experiment of isothermal shrinkage, the initial slope in *Figure 9* is erroneous because the isothermal environment is not made at zero time. Only the significant slopes are denoted in *Figure 9*. This result indicates that time dependence of its isothermal contraction ratio can be described by exponential function.

It can be shown that the two-state model has the same time dependence. By solving equation (4) under the conditions $x = 0$ at $t = 0$ and $dx/dt = 0$ at $t = \infty$, the isothermal contraction ratio at time $t = t$ is given by (see Appendix)

$$\frac{\Delta L(\infty) - \Delta L(t)}{\Delta L(\infty)} = \exp[-(k_f + k_b)t] \qquad (11)$$

and the coefficient a_T is approximated by

$$a_T = k_f + k_b \cong 2A \exp\left(-\frac{\Delta E}{RT}\right) \qquad (12)$$

when $\Delta E \gg Y \cdot s_0 \cdot \Delta l$ and $\Delta E \gg \epsilon - Y \cdot s_0 \cdot \Delta l$. The activation energy ΔE is ~ 66 kcal/mol for our result, which coincides roughly with the value (~40 kcal/mol) obtained from the constant heating rate experiment.

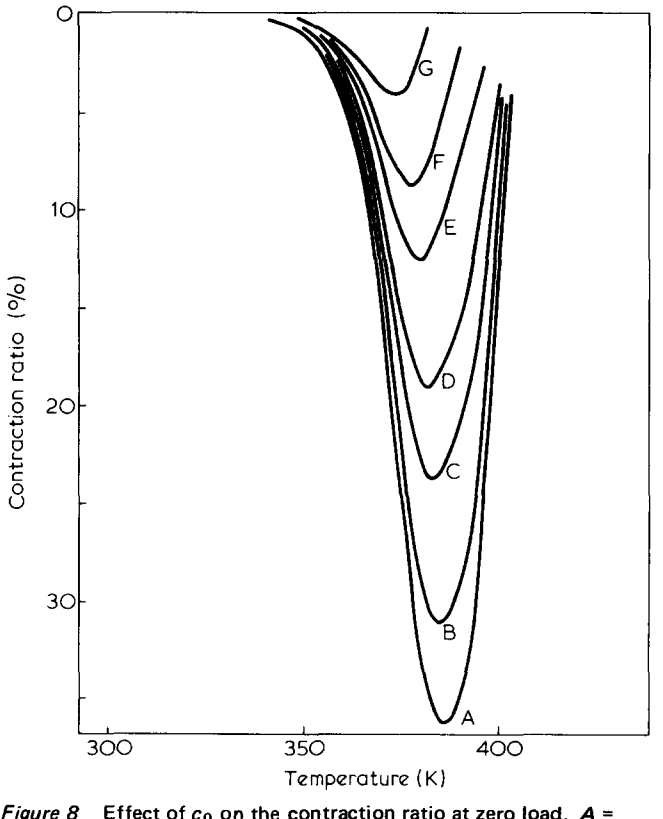

Figure 8 Effect of c_0 on the contraction ratio at zero load, A = 10^{21} (sec^{-1}); ϕ = 1/30 (°C/sec); ΔE = 40 kcal/mol; ϵ = 4.0 kcal/mol. C_0 = A, 50; B, 70; C, 100; D, 120; E, 150; F, 170; G, 200

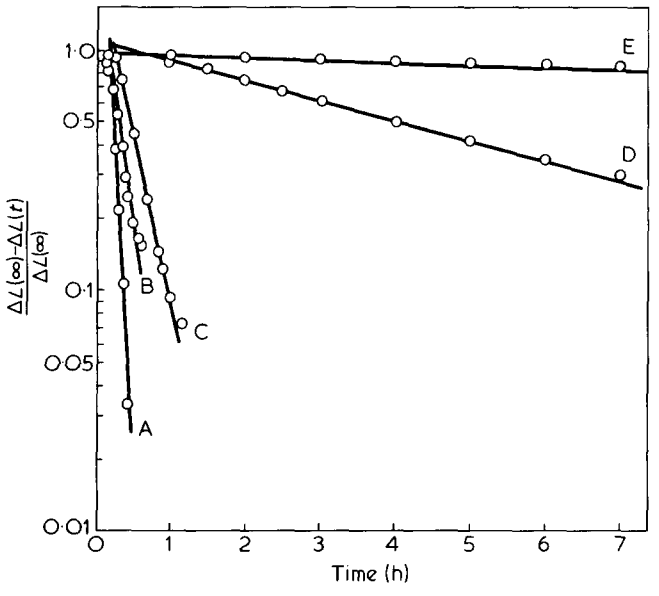

Figure 9 Logarithm of contraction ratio $[\Delta L(\infty) - \Delta L(t)]/\Delta L(\infty)$ of isothermal shrinkage *vs.* time at different temperatures. Sample No. 11 and external load 100 mg. A, 94°C; B, 90°C; C, 80°C; D, 77°C; E, 70°C

Cleereman *et al.*[1] and Andrews[4] have shown that the activation energy is a few hundred kcal/mol for their polystyrene monofilaments. Ueno *et al.*[5] have observed the WLF-type superposition rule in polystyrene films which were drawn above the glass transition temperature. The former monofilaments and the latter uniaxially oriented films recover their undrawn length almost completely. It is difficult to define the original undrawn length of our monofilaments and recovery to original length cannot be discussed. But isothermal shrinkage behaviour of our monofilaments is described by Arrhenius type temperature dependence and activation energy is several tens of kcal/mol. This difference of molecular motions causing thermal shrinkage suggests the difference of the mechanism of vitrification under velocity gradient and of drawing above the glass transition temperature T_g.

Change of Δn *after isothermal shrinkage*

Degree of birefringence after isothermal shrinkage $[\Delta n(\infty)]$ of No. 4 series at 89°C depends on the external load linearly as shown in *Figure 10*. The relationship between the degree of birefringence before isothermal shrinkage ($\Delta n(0)$) and $\Delta n(\infty)$ of No. 3 and No. 4 series is shown in *Figure 11*, where the measured temperature is 89°C and external load is 30 mg. In *Figure 11* the slope of No. 4 sample is smaller; the limiting contraction ratio of this sample is larger (see *Figure 3*).

Changes in the degree of birefringence of polystyrene monofilaments after isothermal shrinkage are also analysed on the basis of the same model. It is not always necessary to assume a submolecule on considering the polarizability tensors. But by using the same model we can discuss the above-mentioned results with the same parameters as those of thermal shrinkage. Principal values of polarizability tensor of a submolecule in the α state are denoted by α_α^1 and α_α^2, which are parallel and perpendicular to fibre axis respectively. In the β state, α_β^1 and α_β^2 are similarly defined. By assuming the applicability of the principle of additivity of polarizability tensors of bulk polymers in the amorphous state, the anisotropy of polarizability $\Delta\alpha(t)$ at time t is represented by:

$$\Delta\alpha(t) = \Delta\alpha(0) - (\Delta\alpha_\beta - \Delta\alpha_\alpha)p_{\beta 0}x(t) \qquad (13)$$

and at time $t = 0$

$$\Delta\alpha(0) = \Delta\alpha_\beta p_{\beta 0} + \Delta\alpha_\alpha p_{\alpha 0} \qquad (14)$$

where $\Delta\alpha_\alpha = \alpha_\alpha^1 - \alpha_\alpha^2$ and $\Delta\alpha_\beta = \alpha_\beta^1 - \alpha_\beta^2$. If anisotropy of polarizability of a submolecule in contracted state is very small and $\Delta\alpha_\alpha \cong 0$, equation (13) leads to

$$\Delta\alpha(t) = \Delta\alpha(0)\,[1 - x(t)] \qquad (15)$$

In the case of a degree of birefringence which is small compared with the average refractive index, Δn is proportional to $\Delta\alpha$, which is derived from Lorentz–Lorenz's formula. Therefore the same equation with equation (15) can be used for Δn instead of $\Delta\alpha$. Degree of birefringence $\Delta n(0)$ and $\Delta n(\infty)$ at temperature T are related to

$$\frac{\Delta n(\infty)}{\Delta n(0)} = \frac{1 + c_0}{\left[1 + \exp\left(\dfrac{\epsilon - 2Y \cdot s_0 \cdot \Delta l}{RT}\right)\right]} \qquad (16)$$

where equation (25) in Appendix is used.

By developing equation (16) with the sufficiently small external stress Y, it is clear that $\Delta n(\infty)$ increases linearly with

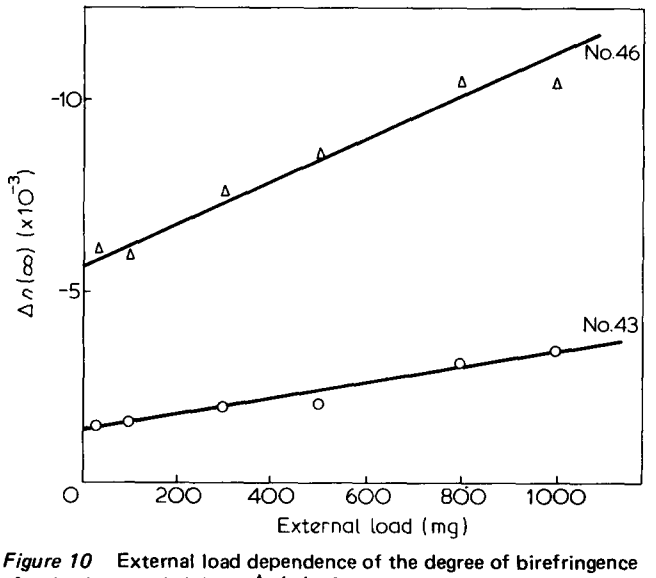

Figure 10 External load dependence of the degree of birefringence after isothermal shrinkage $\Delta n(\infty)$. Samples, No. 4 series and temperature 89°C

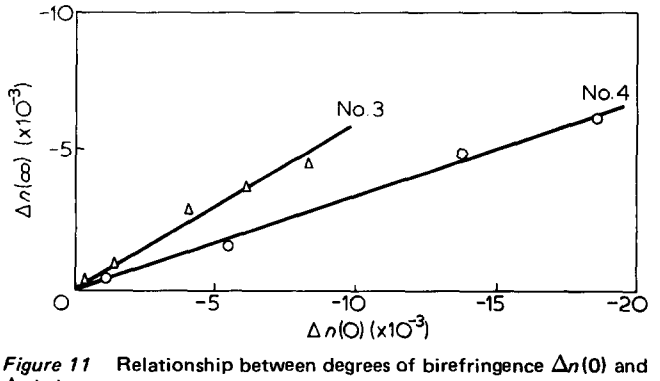

Figure 11 Relationship between degrees of birefringence $\Delta n(0)$ and $\Delta n(\infty)$ before and after isothermal shrinkage, respectively. Samples No. 3 and No.4 series. The external load is 30 mg and temperature is 89°C

increase in Y (see *Figure 10*). Since No. 43 and No. 46 samples have almost the same limiting contraction ratio (44% and 37% in *Figure 3*), the value of the right side of equation (16) is almost constant (see equation 8). Therefore, if $\Delta n(0)$ becomes larger, $\Delta n(\infty)$ increases more steeply with increasing Y. When the limiting contraction ratio

$$\lim_{Y\to 0} \frac{\Delta L_1}{L_0}$$

is large, the value of the right side in equation (16) is small. Accordingly No. 4 samples which have the larger contraction ratios show the smaller slope in *Figure 11*.

From equation (16) and the equation for the contraction ratio $\Delta L_1/L_0$ (see equation (22) in Appendix), the following expression can be obtained at the same temperature ($T = T_1$),

$$C = (\Delta L_1/L_0)/\left[\frac{\Delta n(0) - \Delta n(\infty)}{\Delta n(0)}\right] \qquad (17)$$

From the measurement of the value of the right-hand side of equation (17), order of magnitude of C is ~0.5 for No. 3 and No. 4 samples.

CONCLUSIONS

The thermal shrinkage behaviour of atactic polystyrene monofilaments obtained by our spinning method has been observed by t.m.a. These samples show brittle-to-ductile transition in the vicinity of $\Delta n = -2 \times 10^{-3}$ (under the conditions of a temperature of 20°C and stretching rate of 100%/min) independently of the various spinning conditions.

The contraction ratio decreases linearly with increase in external tensile load.

The limiting contraction ratio

$$\lim_{Y\to 0} \frac{\Delta L_1}{L_0}$$

increases monotonically with increase in $|\Delta n|$ in the brittle region, and decreases more slowly with increase in $|\Delta n|$ in the ductile region. There is a maximum in the vicinity of $\Delta n = -2 \times 10^{-3}$. But its Δn dependence is not so drastic as that of elongation at break.

These results were analysed on the basis of the two-state model in which a submolecule can occupy extended or contracted state. This model interprets the external load dependence of contraction ratio qualitatively. In the brittle region increase of the number of extended submolecules $p_{\beta 0}$ takes prominent effect on

$$\lim_{Y\to 0} \frac{\Delta L_1}{L_0}$$

In the ductile region decrease of energy difference ϵ according to closer oriented packing makes a more important effect than $p_{\beta 0}$.

The time dependence of the isothermal contraction ratio $[\Delta L(\infty) - \Delta L(t)]/\Delta L(\infty)$ is represented by exponential function and Arrhenius type temperature dependence is realized. Its activation energy is several tens of kcal/mol.

The degree of birefringence after isothermal shrinkage $\Delta n(\infty)$ increases linearly with increase in external tensile load.

The degree of birefringence before isothermal shrinkage ($\Delta n(0)$) and $\Delta n(\infty)$ are almost linearly related.

The two-state model is also available to investigate the isothermal shrinkage behaviours of these oriented polystyrene monofilaments.

ACKNOWLEDGEMENT

The authors wish to thank Mr T. Kurita for spinning of polystyrene and the members of Polymer Physics Laboratory in this Research Institute for helpful discussions during the course of this work.

APPENDIX

Derivation of equations (7), (10) and (11)

From the definition of the number fraction $x(t)$ of submolecules, the numbers of submolecules in α and β states are given by

$$p_\alpha(t) = p_{\alpha 0} + p_{\beta 0} x(t) \qquad (18)$$

$$p_\beta(t) = p_{\beta 0}[1 - x(t)] \qquad (19)$$

Using equation (4)

$$\frac{dx(t)}{dt} = (k_f - c_0 k_b) - (k_f + k_b)x(t) \qquad (20)$$

Under the initial and boundary conditions of $x = 0$ at $t = 0$ and $dx/dt = 0$ at $t = t_1$ (or $T = T_1$), we can obtain the solution of equation (20) easily.

$$x(t_1) = \frac{k_f(T_1) - c_0 k_b(T_1)}{k_f(T_1) + k_b(T_1)} \qquad (21)$$

Therefore

$$\frac{\Delta L_1}{L_0} = C\frac{k_f - c_0 k_b}{k_f + k_b} = C\left[1 - \frac{1 + c_0}{\left\{1 + \exp\left(\frac{\epsilon - 2Y \cdot s_0 \cdot \Delta l}{RT_1}\right)\right\}}\right] \qquad (22)$$

where equations (3), (5) and (6) are used. When the external stress is small enough, equation (22) can be developed by $Ys_0\Delta l/RT_1$ and leads to equations (7), (8) and (9) in text.

In the case of a constant heating rate, the time variable can be changed to the temperature variable T by using the heating rate $\phi = dT/dt$. Equation (20) becomes

$$\frac{dx(T)}{dT} = \phi^{-1}[k_f(T) - c_0 k_b(T)] - \phi^{-1}[k_f(T) + k_b(T)]\,x(T)$$

$$= Q(T) - P(T)x(T) \qquad (23)$$

where $P(T) = \phi^{-1}[k_f + k_b]$ and $Q(T) = \phi^{-1}[k_f - c_0 k_b]$. Equation (23) can be solved formally with the elementary method for solving the linear differential equations. With the condition of $x = 0$ at $T = T_0$

$$x(T) = \left\{ \int_{T_0}^{T} Q(T') \exp\left[\int_{T_0}^{T'} P(T'')dT'' \right] dT' \right\} \exp\left[- \int_{T_0}^{T} P(T')dT' \right] \quad (24)$$

and then $\Delta L(T)/L_0$ is given by equation (10) in text.

In the case of the isothermal shrinkage, the parameters k_f and k_b in equation (20) are constant with regard to time t. The solution of equation (20) under the conditions $x = 0$ at $t = 0$ and $dx/dt = 0$ at $t = \infty$ is as follows:

$$x(t) = \frac{k_f - c_0 k_b}{k_f + k_b} \left\{ 1 - \exp[-(k_f + k_b)t] \right\} \quad (25)$$

Using equation (3), we can obtain equation (11).

REFERENCES

1 Cleereman, K. J., Karam, H. J. and Williams, J. L. *Mod. Plast.* 1953, **30**, 119
2 Tanabe, Y. and Kanetsuna, H. *J. Appl. Polym. Sci.* 1978, **22**, 2707
3 Tanabe, Y. and Kanetsuna, H. *J. Appl. Polym. Sci.* 1978, **22**, 1619
4 Andrews, R. D. *J. Appl. Phys.* 1955, **26** 1061
5 Ueno, W., Okuyama, H. and Sadamatsu, S. *Rep. Progr. Polymer Phys. Japan* 1965, **8**, 229
6 Kambe, H. and Kato, T. *Appl. Polym. Symp.* 1973, **20**, 365
7 Kambe, H., Kato, T. and Kochi, M. *J. Macromol. Sci.* 1974, **A8**, 157